

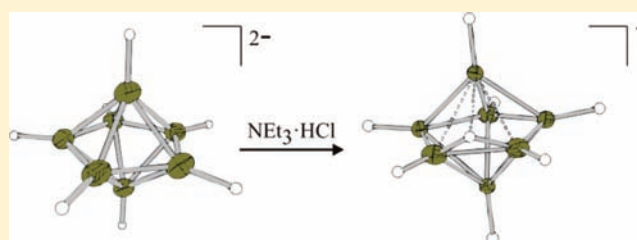
# Syntheses and Crystal Structures of the *closo*-Borates $M_2[B_7H_7]$ and $M[B_7H_8]$ ( $M = PPh_4, PNP,$ and $N(n-Bu_4)$ ): the Missing Crystal Structure in the Series $[B_nH_n]^{2-}$ ( $n = 6-12$ )

Florian Schlüter and Eduard Bernhardt\*

Fachbereich C—Anorganische Chemie, Bergische Universität-GH Wuppertal, Gausstrasse 20, 42097 Wuppertal, Germany

Supporting Information

**ABSTRACT:** Oxidation of  $[N(n-Bu_4)]_2[B_9H_9]$  with oxygen in a mixture of dimethoxyethane and  $CH_2Cl_2$  leads to salts of the  $[B_7H_7]^{2-}$  dianion. This is the first convenient synthesis for a seven-vertex *hydro-closo*-borate anion. Protonation with  $NEt_3 \cdot HCl$  resulted in salts of the  $[B_7H_8]^-$  monoanion. Both *closo*-borate anions were isolated and characterized by  $^1H$ ,  $^1H\{^{11}B\}$ ,  $^{11}B$ , and  $^{11}B\{^1H\}$  NMR spectroscopy. The temperature-dependent  $^1H\{^{11}B\}$ ,  $^{11}B$ , and  $^{11}B\{^1H\}$  NMR spectra of  $[B_7H_8]^-$  were also measured. The structure of  $[B_7H_7]^{2-}$  as well as of  $[B_7H_8]^-$  were determined by single-crystal X-ray diffraction.



## INTRODUCTION

The first *closo*-borate anion  $[B_{10}H_{10}]^{2-}$  was synthesized in 1959.<sup>1</sup> The discovery of other members of the series  $[B_nH_n]^{2-}$  ( $n = 6-12$ ) followed in the next eight years ( $[B_6H_6]^{2-}$ ,<sup>2</sup>  $[B_7H_7]^{2-}$ ,<sup>3</sup>  $[B_8H_8]^{2-}$ ,<sup>3</sup>  $[B_9H_9]^{2-}$ ,<sup>4</sup>  $[B_{11}H_{11}]^{2-}$ ,<sup>4</sup>  $[B_{12}H_{12}]^{2-}$ ,<sup>5</sup>). Reviews with more details about  $[B_6H_6]^{2-}$ ,<sup>6</sup>  $[B_{11}H_{11}]^{2-}$ ,<sup>7</sup> and  $[B_{12}H_{12}]^{2-}$ <sup>8</sup> have been published. Furthermore the crystal structures of *closo*-borates  $[B_6H_6]^{2-}$ ,<sup>9,10</sup>  $[B_8H_8]^{2-}$ ,<sup>11</sup>  $[B_9H_9]^{2-}$ ,<sup>12</sup>  $[B_{10}H_{10}]^{2-}$  (e.g.,  $Cu_2[B_{10}H_{10}]^{13,14}$  and  $Cs[Na(NH_3)_6[B_{10}H_{10}] \cdot NH_3]^{15}$ ),  $[B_{11}H_{11}]^{2-}$ ,<sup>16</sup> and  $[B_{12}H_{12}]^{2-}$  (e.g.,  $K_2[B_{12}H_{12}]^{17}$ ,  $M_2[B_{12}H_{12}]$  and  $M_3[B_{12}H_{12}]$  with  $M = K, Rb, NH_4, Cs^{18}$ ) were determined.<sup>19</sup> The  $[B_7H_7]^{2-}$  anion has not been the subject of a X-ray crystallographic study so far.<sup>20</sup>  $[B_7H_7]^{2-}$  has been partially characterized by  $^{11}B$  NMR, but it has proven to be difficult.<sup>3</sup> The  $^{11}B$  NMR spectrum of the compound was recorded immediately after its preparation, but it was not possible to isolate the  $[B_7H_7]^{2-}$  anion from the solution free of borate impurities,<sup>3</sup> which shows the instability of the dianion. In Scheme 1 the synthesis reported in the literature is shown that yielded the  $[B_7H_7]^{2-}$  anion in eight steps in an overall yield of only 0.008%.

To date there are a lot of theoretically studies<sup>20,22-26</sup> on  $[B_7H_7]^{2-}$  and  $[B_7H_8]^-$ , but only one experimental study.<sup>3</sup>

The labeling of the  $[B_7H_7]^{2-}$  dianion and the  $[B_7H_8]^-$  monoanion is depicted in Figure 1.

The syntheses and the crystal structures of  $[B_7H_7]^{2-}$  and  $[B_7H_8]^-$  are of general interest because of their unique bonding situations and because simple *closo*-borate are valuable starting materials for further borate anions.<sup>27,28</sup> Here we report on an improved synthesis for  $M_2[B_7H_7]$  ( $M = PPh_4$  (tetraphenylphosphonium) and  $PNP$  (Bis-(triphenylphosphine)iminium)). In addition, the monoanion  $[B_7H_8]^-$  was synthesized in good yields. Both anions were extensively

characterized by  $^1H$ ,  $^1H\{^{11}B\}$ ,  $^{11}B$ ,  $^{11}B\{^1H\}$  NMR spectroscopy and X-ray crystallography.

## EXPERIMENTAL SECTION

**Synthesis.**  $[N(n-Bu_4)]_2[B_9H_9]$ .  $Cs_2[B_9H_9]^{4-}$  (3.45 g, 9.27 mmol) was dissolved in 700 mL of 1.6 M NaOH at 333 K.  $[N(n-Bu_4)]HSO_4$  (13.50 g, 39.76 mmol) in 120 mL of 1.6 M NaOH was added under stirring, the resulting colorless precipitate was separated, washed with the mother liquor, and dried in vacuum. Yield: 5.48 g, 9.27 mmol, 100%.

$[PPh_4]_2[B_7H_7]$ . A suspension of  $[N(n-Bu_4)]_2[B_9H_9]$  (1.50 g, 2.53 mmol) in 60 mL of dimethoxyethane was stirred for 15 min at 80 °C. The hot suspension was filtered, and the residue was washed with 45 mL of hot dimethoxyethane and 60 mL of  $CH_2Cl_2$ . Oxygen was then bubbled through the combined solutions for 30 min. The solution was treated with 1 mL of tripropylamine and 60 mL of 0.7 M KOH solution. Organic solvents were removed in a vacuum, and an additional amount of 100 mL of 0.3 M KOH solution was added. After stirring overnight a light yellowish solid was filtered off, and  $[PPh_4]Cl$  (1.42 g, 3.80 mmol) in 20 mL of water was added to the filtrate. The resulting milky mixture was extracted immediately three times with 100 mL of  $CH_2Cl_2$ . The combined organic yellow solutions were dried over  $Na_2SO_4$ , and removal of the  $CH_2Cl_2$  led to a yellow solid, which was washed three times with 40 mL of acetone and dried in vacuum. Yield: 0.71 g, 0.94 mmol, 37%.

$[PPh_4][B_7H_8]$ . This compound was prepared under argon atmosphere, using Schlenk line techniques and dry solvents.  $[PPh_4]_2[B_7H_7]$  (0.10 g, 0.14 mmol) and  $NEt_3 \cdot HCl$  (0.10 g, 0.70 mmol) was placed in a flask under an argon atmosphere, and 20 mL of dry MeCN was added under stirring. The solution was stirred for 15 min, and then the solvent was removed in vacuum. Twenty milliliters of dry MeCN was added again and removed

Received: December 6, 2010

Published: February 22, 2011

after 15 min of stirring. The resulting faintly yellow solid was dried in vacuum overnight. A 100 mL portion of H<sub>2</sub>O was added, and the suspension was stirred for 15 min. The solid was separated, washed again with 50 mL of H<sub>2</sub>O, and dried in vacuum. Yield: 0.06 g, 0.13 mmol, 93%; (Yield based on NMR data 100%).

[PNP]<sub>2</sub>[B<sub>7</sub>H<sub>7</sub>]. [PPh<sub>4</sub>]<sub>2</sub>[B<sub>7</sub>H<sub>7</sub>] (0.23 g, 0.30 mmol) in 40 mL of CH<sub>2</sub>Cl<sub>2</sub> and 1 mL of NEt<sub>3</sub> was added to a solution [PNP]Cl (0.34 g, 0.60 mmol) in 20 mL of CH<sub>2</sub>Cl<sub>2</sub> and 1 mL of NEt<sub>3</sub>. The reaction solution was evaporated to dryness, and the resulting solution was treated with 1 g K<sub>2</sub>CO<sub>3</sub> in 100 mL of H<sub>2</sub>O. The suspension was stirred for 30 min, the yellow solid was separated, washed three times with 20 mL of H<sub>2</sub>O, and dried in vacuum. Yield: 0.35 g, 0.30 mmol, 95%.

[PNP][B<sub>7</sub>H<sub>8</sub>]. This compound was prepared under an argon atmosphere, using Schlenk line techniques and dry solvents. [PNP]<sub>2</sub>[B<sub>7</sub>H<sub>7</sub>] (0.16 g, 0.14 mmol) and NEt<sub>3</sub>·HCl (0.10 g, 0.70 mmol) were placed in a flask under an argon atmosphere, and 20 mL of dry MeCN was added under stirring. The reaction solution was stirred for 15 min, and the solvent was removed in vacuum. Twenty milliliters of dry MeCN was added again and removed after 15 min of stirring. The resulting faintly yellow solid was dried in vacuum overnight. A 300 mL portion of H<sub>2</sub>O was added, and the suspension was stirred for 15 min. The solid was separated, washed again with 250 mL of H<sub>2</sub>O, and dried in vacuum. Yield: 0.08 g, 0.13 mmol, 93%; (Yield based on NMR data 100%).

**Chemicals.** All chemicals were obtained from commercial sources. Solvents were dried by distillation and stored in flasks equipped with valves with PTFE stems (Young, London) over molecular sieves (4 Å) under an argon atmosphere. Cs[B<sub>3</sub>H<sub>8</sub>]<sup>21</sup> and Cs<sub>2</sub>[B<sub>9</sub>H<sub>9</sub>]<sup>4</sup> were prepared according to a known procedures.

**Crystal Structure Determination.** Crystals were centered on an Oxford Diffraction Gemini E Ultra diffractometer, equipped with

**Scheme 1. Synthesis of [B<sub>7</sub>H<sub>7</sub>]<sup>2-</sup>, Starting from Na[BH<sub>4</sub>]; Literature: Step I, II,<sup>21</sup> Step III, IV,<sup>4</sup> and Step V, VI, VII, and VIII<sup>3</sup>**

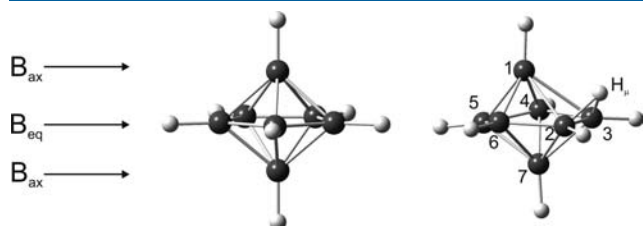
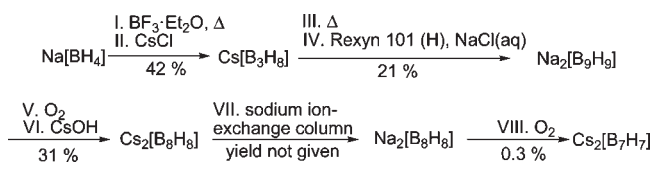


**Figure 1.** Labeling of the positions of the [B<sub>7</sub>H<sub>7</sub>]<sup>2-</sup> and [B<sub>7</sub>H<sub>8</sub>]<sup>-</sup>.

a 2K × 2K EOS CCD area detector, a four-circle κ goniometer, an Oxford Instruments Cryojet, and sealed-tube Enhanced (Mo) and the Enhanced Ultra (Cu) sources. For the data collection, the Cu source emitting monochromated Cu Kα radiation (λ = 1.54184 Å) or Mo Kα radiation (λ = 0.71073 Å) were used. The diffractometer was controlled by the CrysAlisPro Graphical User Interface (GUI) software.<sup>29</sup> Processing of the raw data, scaling of diffraction data, and the application of an empirical absorption correction was completed by using the CrysAlisPro program.<sup>34</sup>

Crystallographic data for [N(*n*-Bu<sub>4</sub>)]<sub>2</sub>[B<sub>7</sub>H<sub>7</sub>] (CCDC-801375), [PPh<sub>4</sub>]<sub>2</sub>[B<sub>7</sub>H<sub>7</sub>]·CH<sub>2</sub>Cl<sub>2</sub> (CCDC-801377), [PPh<sub>4</sub>]<sub>2</sub>[B<sub>7</sub>H<sub>7</sub>]·1.36CH<sub>3</sub>CN (CCDC-801376), [PNP]<sub>2</sub>[B<sub>7</sub>H<sub>7</sub>]·3CH<sub>3</sub>CN (CCDC-801373), [*p*-Ph<sub>3</sub>P-C<sub>6</sub>H<sub>4</sub>PPh<sub>3</sub>]<sub>2</sub>[PPh<sub>4</sub>]<sub>2</sub>[B<sub>7</sub>H<sub>7</sub>]·6.5H<sub>2</sub>O (CCDC-801378), [N(*n*-Bu<sub>4</sub>)]-[B<sub>7</sub>H<sub>8</sub>] (CCDC-801374), and [PNP][B<sub>7</sub>H<sub>8</sub>] (CCDC-801372) have been deposited with the Cambridge Crystallographic Data Centre, 12 Union Road, Cambridge CB21EZ, U.K. Copies of the data can be obtained on request from www.ccdc.cam.ac.uk/data\_request/cif; (Fax +44-1223-336-033, E-mail: deposit@ccdc.cam.ac.uk).

**NMR.** A Bruker ARX III 600 spectrometer (600.13 MHz for <sup>1</sup>H and 192.55 MHz for <sup>11</sup>B) and dichloromethane-*d*<sub>2</sub> as solvent were used. External standards are SiMe<sub>4</sub> (δ(<sup>1</sup>H) = 0 ppm) and BF<sub>3</sub>·OEt<sub>2</sub> (δ(<sup>11</sup>B) = 0 ppm).

**Theoretical Calculations.** Quantum chemical calculations were performed to support the experimental results. Density functional theory (DFT) calculations<sup>30</sup> were done with the B3LYP-Method.<sup>31–33</sup> The 6-311++G(d,p) basis set was used as implemented in the Gaussian03 program suite.<sup>34</sup> The shielding constants (GIAO)<sup>35–39</sup> and the coupling constants were calculated as described in the literature.<sup>40–43</sup> Intrinsic reaction path (IRC) calculations were performed for all transition states.<sup>44,45</sup>

## RESULTS AND DISCUSSION

**Synthesis.** Oxidation of Na<sub>2</sub>[B<sub>9</sub>H<sub>9</sub>] in dimethoxyethane with oxygen results in [B<sub>8</sub>H<sub>8</sub>]<sup>2–3</sup> as main product, whereas the oxidation of [N(*n*-Bu<sub>4</sub>)]<sub>2</sub>[B<sub>9</sub>H<sub>9</sub>] in a mixture of dimethoxyethane/CH<sub>2</sub>Cl<sub>2</sub> gives [B<sub>7</sub>H<sub>7</sub>]<sup>2–</sup> as main product (Scheme 2).

Other *closo*-borates, for example, [B<sub>12</sub>H<sub>12</sub>]<sup>2–</sup>, [B<sub>10</sub>H<sub>10</sub>]<sup>2–</sup>, [B<sub>6</sub>H<sub>6</sub>]<sup>2–</sup>/[B<sub>6</sub>H<sub>7</sub>]<sup>-</sup>, and the until now unknown species [B<sub>7</sub>H<sub>8</sub>]<sup>-</sup> were observed in the NMR spectrum of the crude product mixture after treatment of a solution of [N(*n*-Bu<sub>4</sub>)]<sub>2</sub>[B<sub>9</sub>H<sub>9</sub>] with oxygen in dimethoxyethane/CH<sub>2</sub>Cl<sub>2</sub> for 10 min (Figure 2). Dissolving [N(*n*-Bu<sub>4</sub>)]<sub>2</sub>[B<sub>9</sub>H<sub>9</sub>] in a mixture of dimethoxyethane/CH<sub>2</sub>Cl<sub>2</sub> (1.75: 1) is accompanied by a light red coloration of the solution. Oxygen is bubbled through the solution for 30 min. After 3 min the solution becomes intensively red, and after 6 min a nearly black solution is

**Scheme 2. Synthesis of [B<sub>7</sub>H<sub>7</sub>]<sup>2-</sup>, Starting from Na[BH<sub>4</sub>]; Literature: Step I, II<sup>21</sup> and Step III,<sup>4</sup> Step IV–VI This Work**

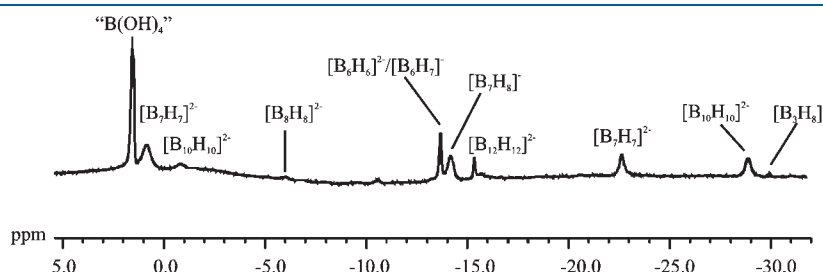
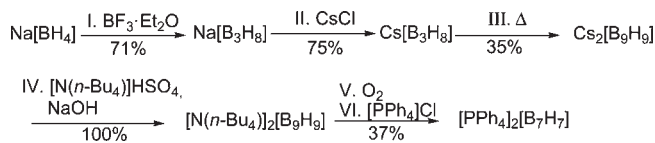


**Figure 2.** <sup>11</sup>B{<sup>1</sup>H} NMR-spectrum of the reaction mixture in CD<sub>2</sub>Cl<sub>2</sub> at 300 K.

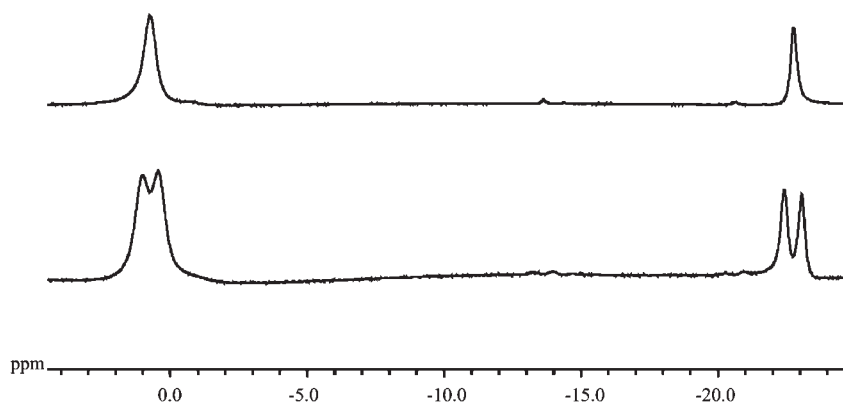


Figure 3.  $^{11}\text{B}$  and  $^{11}\text{B}\{^1\text{H}\}$  NMR spectra of  $[\text{PPh}_4]_2[\text{B}_7\text{H}_7]$  in  $\text{CD}_2\text{Cl}_2$ .

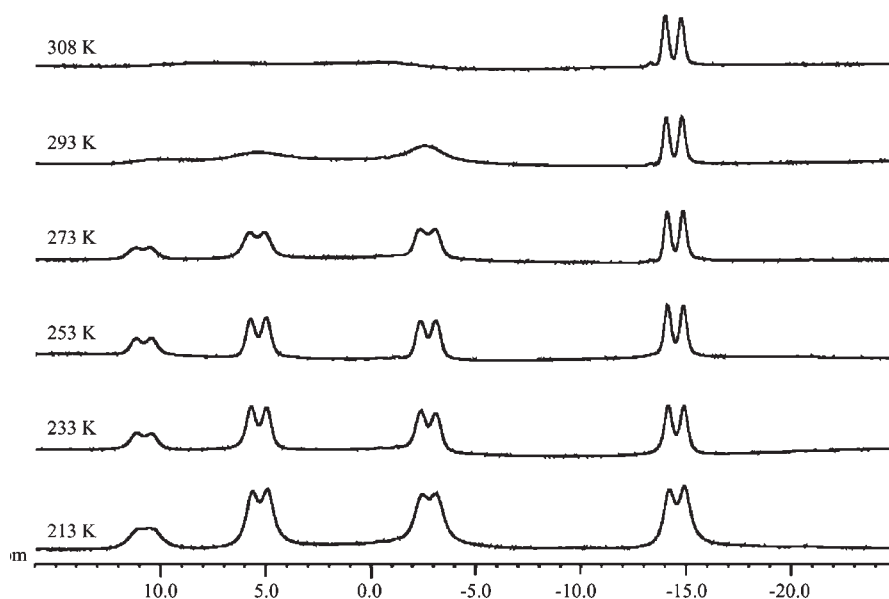


Figure 4.  $^{11}\text{B}$  NMR spectra of  $[\text{B}_7\text{H}_8]^-$  in  $\text{CD}_2\text{Cl}_2$  at various temperatures.

Table 1. Calculated and Experimental NMR Data for  $[\text{PPh}_4]_2[\text{B}_7\text{H}_7]$  (at 300 K) and  $[\text{PPh}_4][\text{B}_7\text{H}_8]$  (at 233 K), Measurement in  $\text{CD}_2\text{Cl}_2$

	$[\text{PPh}_4]_2[\text{B}_7\text{H}_7]$		$[\text{PPh}_4][\text{B}_7\text{H}_8]$	
	experimental	calculated <sup>a</sup>	experimental <sup>b</sup>	calculated <sup>a</sup>
$\delta(^{11}\text{B})$ , ppm	0.7 {110}, B2–B6	−4.6 {117}	10.8 {136}, B5	11.9 {138}
$\{^1J(^{11}\text{B},^1\text{H})$ , Hz}	−22.8 {124}, B1, B7	−29.1 {114}	5.4 {140}, B4, B6	2.6 {137}
			−2.7 {141}, B2, B3	−4.0 {134}
			−14.5 {142}, B1, B7	−14.3 {137} <sup>c</sup>
$\delta(^1\text{H})$ , ppm	H2–H6, 3.47	3.48	H2, H3 4.01, t {11 H4, H6}	4.24 {10}
$\{^3J(^1\text{H},^1\text{H})$ , Hz}	H1, H7, −0.95	−0.65	H5, 3.96, s, br	4.40
			H4, H6, 3.87, s, br	4.11
			H8, 0.90, t {16 H2, H3}	0.01 {14}
			H1, H7, −0.46, s	0.06 <sup>c</sup>

<sup>a</sup> GIAO//B3LYP/6-311++g(d,p), referenced against  $\text{BF}_3 \cdot \text{OEt}_2$  ( $\delta(^{11}\text{B}) = 0$  ppm)  $\delta(^{11}\text{B}) = 101.63 - \sigma(^{11}\text{B})$  and  $\text{Me}_4\text{Si}$  ( $\delta(^1\text{H}) = 0$  ppm),  $\delta(^1\text{H}) = 31.97 - \sigma(^1\text{H})$ . <sup>b</sup> For more details see the Supporting Information. <sup>c</sup> Averaged values for B1/B7 and H1/H7.

obtained. Within the next 15 min the solution is almost decolorized resulting in a slightly yellow color. Basic water is added, and the organic solvents are removed in a vacuum. Under basic

conditions the *closo*-borate  $[\text{B}_7\text{H}_7]^{2-}$  is stable in water; that allows the separation of the various *closo*-borate. Tetrabutylammonium salts of  $[\text{B}_6\text{H}_6]^{2-}$  and  $[\text{B}_7\text{H}_7]^{2-}$  are soluble in water; in contrast to

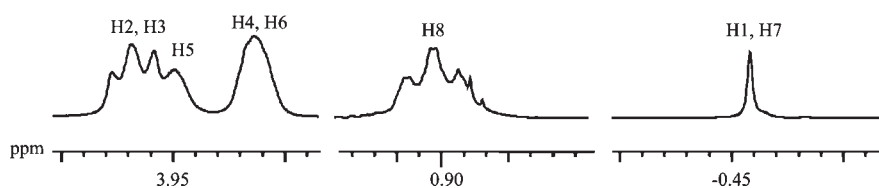


Figure 5.  $^1\text{H}\{^{11}\text{B}\}$  NMR spectrum of  $[\text{B}_7\text{H}_8]^-$  in  $\text{CD}_2\text{Cl}_2$  at 233 K.

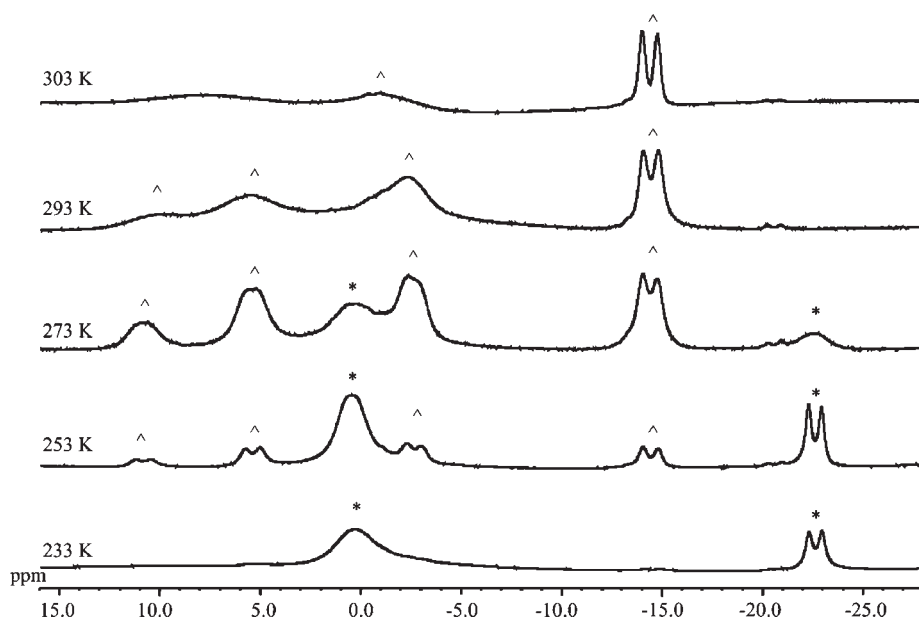


Figure 6.  $^{11}\text{B}$  NMR spectra of the mixture of  $[\text{B}_7\text{H}_7]^{2-}$  and  $\text{NEt}_3 \cdot \text{HCl}$  in  $\text{CD}_2\text{Cl}_2$  at various temperatures; \* =  $[\text{B}_7\text{H}_7]^{2-}$ , ^ =  $[\text{B}_7\text{H}_8]^-$ .

this  $[\text{B}_{12}\text{H}_{12}]^{2-}$  and  $[\text{B}_{10}\text{H}_{10}]^{2-}$  are insoluble. Both borates,  $[\text{B}_6\text{H}_6]^{2-}$  and  $[\text{B}_7\text{H}_7]^{2-}$ , are converted to the corresponding tetraphenylphosphonium salts with  $[\text{PPh}_4]\text{Cl}$ . Extraction of the *closo*-borates with  $\text{CH}_2\text{Cl}_2$  and removal of the solvent under vacuum results in a yellow solid. Washing with acetone leads to pure product:  $[\text{PPh}_4]_2[\text{B}_6\text{H}_6]$ ,  $[\text{PPh}_4][\text{B}_6\text{H}_7]$ , and excess  $[\text{PPh}_4]\text{Cl}$  are soluble in acetone whereas  $[\text{PPh}_4]_2[\text{B}_7\text{H}_7]$  is insoluble. In contrast to the known procedure using  $\text{Na}_2[\text{B}_8\text{H}_8]$  as starting material the isolation of salts of the  $[\text{B}_7\text{H}_7]^{2-}$  anion in yields as high as 37% starting from  $[\text{N}(n\text{-Bu}_4)]_2[\text{B}_9\text{H}_9]$  is possible. The overall yield is 7%, this is about 900 times better than the published synthesis.

The cation exchange with Bis(triphenylphosphine)iminium chloride ( $[\text{PNP}]\text{Cl}$ )<sup>46</sup> to yield  $[\text{PNP}]_2[\text{B}_7\text{H}_7]$  is performed under basic conditions in  $\text{CH}_2\text{Cl}_2$ . The organic solvent is removed in a vacuum and the resulting yellow solid is washed with basic water to remove excess of  $[\text{PNP}]\text{Cl}$ . Stirring of  $\text{M}_2[\text{B}_7\text{H}_7]$  in  $\text{CH}_2\text{Cl}_2$  and DBU (DBU = 1,8-Diazabicyclo[5.4.0]undec-7-ene, a strong base), leads to a very slowly reaction from  $[\text{B}_7\text{H}_7]^{2-}$  to give  $2\text{-}[\text{B}_7\text{H}_6\text{Cl}]^{2-}$ .

Protonation of  $\text{M}_2[\text{B}_7\text{H}_7]$  ( $\text{M} = \text{PNP}^+$ ,  $\text{PPh}_4^+$ ) with  $\text{NEt}_3 \cdot \text{HCl}$  in MeCN leads to  $[\text{B}_7\text{H}_8]^-$  (see also eq 1). The deep yellow color vanished immediately after addition of  $\text{NEt}_3 \cdot \text{HCl}$  in MeCN to a solution of  $\text{M}_2[\text{B}_7\text{H}_7]$  in MeCN. Removal of the solvent in vacuum and washing with water gives  $\text{M}[\text{B}_7\text{H}_8]$  in quantitative yield as colorless solid. Slow diffusion of  $\text{Et}_2\text{O}$  ( $\text{Et}_2\text{O} = \text{diethyl ether}$ ) into a saturated  $\text{CH}_2\text{Cl}_2$  solution leads to colorless crystals, which can be separated and dried to yield  $\text{M}[\text{B}_7\text{H}_8]$  in nearly quantitative yield.

**NMR Spectroscopy.** The NMR spectrum of the reaction mixture after treating the solution for 10 min with oxygen is

presented below (Figure 2) and shows the various *closo*-borates and other boron compounds.

$[\text{B}_{12}\text{H}_{12}]^{2-}$  (−15.3 ppm),  $[\text{B}_{10}\text{H}_{10}]^{2-}$  (−28.9, −0.8 ppm), and  $[\text{B}_6\text{H}_6]^{2-}/[\text{B}_6\text{H}_7]^-$  (−13.7 ppm) as well as traces of  $[\text{B}_8\text{H}_8]^{2-}$  (−6.0 ppm) are observed. In addition, the *closo*-borate  $[\text{B}_7\text{H}_7]^{2-}$  (0.8, −22.7 ppm) and the monoanion  $[\text{B}_7\text{H}_8]^-$  (−14.2 ppm, for the two axial atoms) can be assigned.

The  $^{11}\text{B}$  NMR spectrum of the yellow  $[\text{PPh}_4]_2[\text{B}_7\text{H}_7]$  shows two doublets with relative intensities of 5 and 2 (Figure 3). These data are consistent with a pentagonal bipyramid, which is in agreement with the results of the crystal structure analysis.

The spectrum of the  $[\text{B}_7\text{H}_7]^{2-}$  anion depicted in Figure 3 is in agreement to the data described in the literature.<sup>3</sup> The  $^{11}\text{B}$  NMR spectrum of  $[\text{B}_7\text{H}_8]^-$  shows at room temperature only one doublet and very broad signals between −3 ppm and 12 ppm. Four doublets can be observed if the solution is cooled down (Figure 4). At 273 K the equatorial boron atoms of the pentagonal bipyramid of  $[\text{B}_7\text{H}_8]^-$  are visible in the  $^{11}\text{B}$  NMR. At 253 K three well resolved doublets with intensities of 2:2:1 are determined at −2.7, 5.5, and 10.8 ppm.

The rotation of the additional proton around the 5 equatorials boron atoms in solution can be “frozen” at lower temperatures. This confirms the shown spectra above. The oscillation of the bridging proton upward and downward to the five ring could not stopped, which indicates the doublet at −14.5 ppm and the missing further split-up for the axial boron atoms.

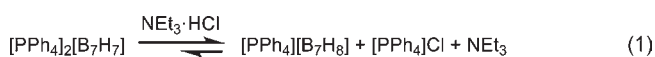
At 233 K each proton of  $[\text{B}_7\text{H}_8]^-$  in  $^1\text{H}\{^{11}\text{B}\}$  NMR spectra can be assigned. The data are summarized in Table 1, and details of the  $^1\text{H}\{^{11}\text{B}\}$  NMR spectra are presented in Figure 5 (for more details see the Supporting Information).

**Table 2.** Crystallographic Data for  $[N(n\text{-Bu}_4)]_2[\text{B}_7\text{H}_7]$  (1),  $[\text{PPh}_4]_2[\text{B}_7\text{H}_7] \cdot \text{CH}_2\text{Cl}_2$  (2),  $[\text{PPh}_4]_2[\text{B}_7\text{H}_7] \cdot 1.36\text{CH}_3\text{CN}$  (3),  $[\text{PNP}]_2[\text{B}_7\text{H}_7] \cdot 3\text{CH}_3\text{CN}$  (4), and  $[p\text{-Ph}_3\text{PC}_6\text{H}_4\text{PPh}_3][\text{PPh}_4]_2[\text{B}_7\text{H}_7]_2 \cdot 6.5\text{H}_2\text{O}$  (5)

	1	2	3	4	5 <sup>c</sup>
temperature, K	110	150	150	150	150
space group	$P2_1/n$ (No. 14)	$P\bar{1}$ (No. 2)	$P\bar{1}$ (No. 2)	$P2_1/n$ (No. 14)	$P\bar{1}$ (No. 2)
color	colorless	yellow	yellow	yellow	yellow
$a$ , Å	10.4637(13)	10.9142(3)	11.5410(5)	10.51780(6)	13.0797(6)
$b$ , Å	51.163(3)	12.2269(4)	12.8777(6)	49.7055(3)	13.6258(7)
$c$ , Å	21.884(3)	18.6005(5)	16.0317(4)	13.58759(7)	14.3517(4)
$\alpha$ , deg	90	78.570(3)	84.993(3)	90	105.425(4)
$\beta$ , deg	95.632(10)	81.762(2)	73.140(3)	95.3820(5)	95.202(3)
$\gamma$ , deg	90	72.257(3)	87.575(4)	90	117.582(5)
cell volume, Å <sup>3</sup>	11659(2)	2308.06(12)	2271.18(15)	7072.17(7)	2115.89(16)
$Z$	12	2	2	4	1
density (calculated), g cm <sup>-3</sup>	0.970	1.219	1.195	1.207	1.231
absorption coefficient, mm <sup>-1</sup>	0.367	0.245	1.134	1.364	1.284
wavelength, Å	1.54184	0.71073	1.54184	1.54184	1.54184
measured $\Theta$ -Area, deg	$3.29 \leq \theta \leq 45.04$	$3.00 \leq \theta \leq 29.84$	$3.45 \leq \theta \leq 61.12$	$3.39 \leq \theta \leq 66.37$	$3.30 \leq \theta \leq 61.26$
completeness to $\theta/d$	97.9%/44.5°/1.1 Å	99.8%/26.4°/0.8 Å	98.5%/58.9°/0.9 Å	99.6%/65.1°/0.85 Å	99.8%/58.9°/0.9 Å
reflections:measured/independent/observed. $[I > 2\sigma(I)]$	12984/a/6942	18297/10862/9046	11550/6729/5141	23294/12275/11534	10819/6375/5315
$R(\text{int})/R(\sigma)$	a/0.1387	0.0163/0.0285	0.0171/0.0240	0.0156/0.0216	0.0179/0.0250
various parameters/restraints	1109/801	575/1	572/0	901/48	597/22
goodness-of-fit on $F^2$ /restrained goodness-of-fit	0.994/0.983	1.023/1.023	1.022/1.022	1.009/1.021	1.063/1.062
$R_1$ observed/all	0.1074/0.1790	0.0416/0.0529	0.0396/0.0546	0.0403/0.0425	0.0328/0.0404
$wR_2$	0.3067	0.1076	0.1068	0.1088	0.0874
largest diff. peak and hole, e Å <sup>-3</sup>	0.378 and -0.303	0.361 and -0.497	0.382 and -0.259	0.382 and -0.259	0.326 and -0.321
$a, b^b$	0.1832/0.00	0.0459/1.0734	0.0436/0.4675	0.0561/3.7717	0.0472/0.3756
CCDC	801375	801377	801376	801373	801378

<sup>a</sup> Twins in agreement with  $(-1\ 0\ 0, 0\ -1\ 0, 0.41\ 0\ 1)$ , percentage of the second component 0.3003(16). <sup>b</sup>  $w = 1/[\sigma^2(F_o^2) + (aP)^2 + bP]$ , with  $P = (\max(F_o^2, 0) + 2F_c^2)/3$ . <sup>c</sup> Extinction coefficient: 0.00055(16).

Instead of this a protonation of  $[\text{PPh}_4]_2[\text{B}_7\text{H}_7]$  with  $\text{NEt}_3 \cdot \text{HCl}$  in situ leads to some interesting results in the <sup>11</sup>B NMR spectra (eq 1 shows the formation of the monoanion  $[\text{B}_7\text{H}_8]^-$ ).



The following investigation of the in situ generated  $[\text{B}_7\text{H}_8]^-$  anion in a solution of the  $[\text{B}_7\text{H}_7]^{2-}$  and  $\text{NEt}_3 \cdot \text{HCl}$  in  $\text{CD}_2\text{Cl}_2$  by NMR spectroscopy is summarized in Figure 6.

Because of the low solubility of  $\text{Et}_3\text{N} \cdot \text{HCl}$  in  $\text{CH}_2\text{Cl}_2$  at low temperatures the equilibrium of the dianion  $[\text{B}_7\text{H}_7]^{2-}$  with its protonated form  $[\text{B}_7\text{H}_8]^-$  is shifted to the dianion as evident from the <sup>11</sup>B NMR spectra in Figure 6. The <sup>11</sup>B chemical shifts are in agreement with the reported values for  $C_{2v}$  symmetry.<sup>24</sup> The NMR spectroscopic data of the compounds  $[\text{PPh}_4]_2[\text{B}_7\text{H}_7]$  and  $[\text{PPh}_4][\text{B}_7\text{H}_8]$  are summarized in Table 1 (for further details see the Supporting Information). Assignment of the boron atoms occurs with them in Figure 1.

**Crystal Structures of Salts of the  $[\text{B}_7\text{H}_7]^{2-}$  Anion.** Until now the crystal structure of  $[(\text{C}_5\text{H}_5\text{N})_2\text{CH}_2][\text{B}_7\text{Br}_7]$  is the only example for a *closo*-heptaborate that was structurally characterized.<sup>47</sup> However, in the sodium boride  $\text{Na}_3\text{B}_{20}$  *closo*-B<sub>7</sub> and -B<sub>6</sub> units were observed.<sup>48,49</sup> Structurally related compounds, which show a pentagonal bipyramid, are, for example, *closo*- $[\text{CB}_6\text{H}_7]^-$  and its derivatives,<sup>50,51</sup> *closo*-C<sub>2</sub>B<sub>5</sub>H<sub>7</sub>,<sup>52</sup> (1,3-Diboroly) ruthenium triple-decker complexes<sup>53</sup> and metalladecaboranes.<sup>54</sup> The unknown and missing crystal structure of  $[\text{B}_7\text{H}_7]^{2-}$  in the series of  $[\text{B}_n\text{H}_n]^{2-}$  ( $n = 6-12$ )

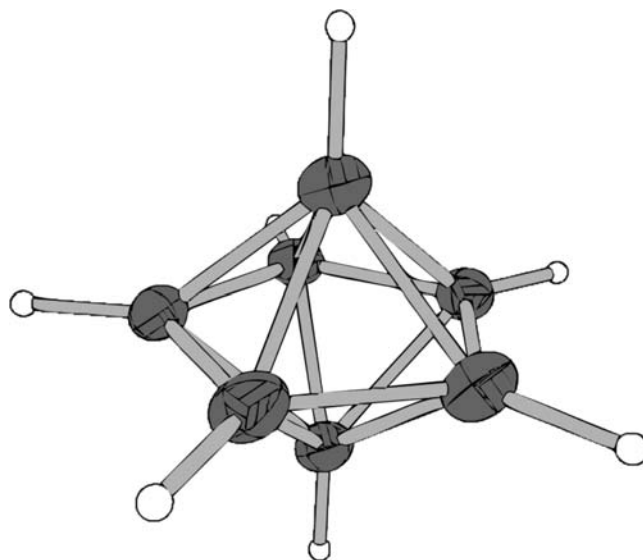


**Figure 7.** Structure of the  $[\text{B}_7\text{H}_7]^{2-}$  anion in  $[\text{PPh}_4]_2[\text{B}_7\text{H}_7] \cdot \text{CH}_2\text{Cl}_2$  with 50% probability thermal ellipsoids for the B atoms.

of *closo*-borates was determined. Various attempts to crystallize the anion  $[\text{B}_7\text{H}_7]^{2-}$  led to different crystals with different structures, solvates, and polymorphs. Also various cations were used. An overview is given in Table 2 (for more details see the Supporting Information).

**Table 3. Overview on the Bond Length in the  $[\text{B}_7\text{H}_7]^{2-}$  Anion with Various Cations: Experimental (Averaged) and Calculated Values**

compound	<i>t</i> , K	$d(\text{B}_{\text{ax}}-\text{B}_{\text{eq}})_{\text{av}}$ , Å <sup>c</sup>	$d(\text{B}_{\text{eq}}-\text{B}_{\text{eq}})_{\text{av}}$ , Å
$[\text{N}(n\text{-Bu}_4)]_2[\text{B}_7\text{H}_7]$	110	1.821{2} (10)	1.649{5} (10)
$[\text{PPh}_4]_2[\text{B}_7\text{H}_7] \cdot \text{CH}_2\text{Cl}_2$	150	1.821{2} (2)	1.6518{10} (20)
$[\text{PPh}_4]_2[\text{B}_7\text{H}_7] \cdot 1.36\text{CH}_3\text{CN}$	150	1.816{2} (3)	1.643{7} (3)
$[\text{Ph}_3\text{PC}_6\text{H}_4\text{PPh}_3][\text{PPh}_4]_2[\text{B}_7\text{H}_7]_2 \cdot 6.5\text{H}_2\text{O}$	150	1.819{4} (3)	1.651{3} (3)
$[\text{PNP}]_2[\text{B}_7\text{H}_7] \cdot 3\text{CH}_3\text{CN}$	150	1.8185{16} (20)	1.643{3} (2)
calculated <sup>a</sup>		1.831	1.656
calculated <sup>b</sup>		1.817	1.651

<sup>a</sup> B3LYP/6-311++g(d,p). <sup>b</sup> MP2(FULL)/6-31G\*. <sup>c</sup> Values on average, calculated with Origin 7G SR2 (v7.0394), in brackets: error of the measurement; in curly brackets: statistical error.

**Table 4. Crystallographic Data for  $[\text{N}(n\text{-Bu}_4)][\text{B}_7\text{H}_8]$  and  $[\text{PNP}][\text{B}_7\text{H}_8]$** 

	$[\text{N}(n\text{-Bu}_4)][\text{B}_7\text{H}_8]$	$[\text{PNP}][\text{B}_7\text{H}_8]$
temperature, K	100	150
space group	$P4_1$ (No. 76)	$P2_1/c$ (No. 14)
color	colorless	colorless
<i>a</i> , Å	10.9833(3)	13.13263(11)
<i>b</i> , Å	10.9833	19.66419(16)
<i>c</i> , Å	37.4965(11)	13.54186(10)
$\beta$ , deg	90	90.2086(7)
cell volume, Å <sup>3</sup>	4523.3(2)	3497.06(5)
<i>Z</i>	8	4
density (calculated), g cm <sup>-3</sup>	0.958	1.182
absorption coefficient, mm <sup>-1</sup>	0.049	1.314
wavelength, Å	0.71073	1.54184
measured $\Theta$ -Area, deg	$3.29 \leq \theta \leq 28.61$	$3.37 \leq \theta \leq 62.49$
completeness to $\theta/d$	99.6%/26.4°/0.8 Å	99.9%/62.4°/0.87 Å
reflexes: measured/independent/observed. [ $I > 2\sigma(I)$ ]	16309/9879/8515	18317/5557/5109
$R(\text{int})/R(\sigma)$	0.0218/0.0372	0.0199/0.0177
various parameters/restraints	462/8	463/0
goodness-of-fit an $F^2$ /restrained goodness-of-fit	1.014/1.013	1.051/1.051
$R_1$ observed/all	0.0563/0.0672	0.0331/0.0360
$wR_2$	0.1508	0.0902
extinction coefficient		0.00033(6)
largest diff. peak and hole, e Å <sup>-3</sup>	0.292 and -0.206	0.292 and -0.298
<i>a</i> , <i>b</i> <sup>a</sup>	0.0728/1.4977	0.0442/1.1698
CCDC	801374	801372

<sup>a</sup>  $w = 1/[\sigma^2(F_o^2) + (aP)^2 + bP]$ , with  $P = (\max(F_o^2, 0) + 2F_c^2)/3$ .

$[\text{N}(n\text{-Bu}_4)]_2[\text{B}_7\text{H}_7]$  (Scheme 2, step V) crystallized from water under basic conditions as colorless small needles (for more details see the Supporting Information). Hence, all data sets measured, even with Cu  $K_{\alpha}$  X-ray, were of relatively poor quality.

Yellow crystals of  $[\text{PPh}_4]_2[\text{B}_7\text{H}_7] \cdot \text{CH}_2\text{Cl}_2$  were obtained by diffusion of Et<sub>2</sub>O into a solution of  $[\text{PPh}_4]_2[\text{B}_7\text{H}_7]$  in CH<sub>2</sub>Cl<sub>2</sub>, and a view of the anion is shown in Figure 7.

Crystals of  $[\text{PPh}_4]_2[\text{B}_7\text{H}_7] \cdot 1.36\text{CH}_3\text{CN}$  were obtained by diffusion of Et<sub>2</sub>O into a solution of  $[\text{PPh}_4]_2[\text{B}_7\text{H}_7]$  in CH<sub>3</sub>CN.

After addition of  $[p\text{-Ph}_3\text{PC}_6\text{H}_4\text{PPh}_3]\text{Br}_2^{55}$  in water to  $[\text{PPh}_4]_2[\text{B}_7\text{H}_7]$  in acetonitrile and evaporation of the acetonitrile  $[p\text{-Ph}_3\text{PC}_6\text{H}_4\text{PPh}_3][\text{PPh}_4]_2[\text{B}_7\text{H}_7]_2 \cdot 6.5\text{H}_2\text{O}$  crystallized from the mother liquor at 276 K.

Crystals of  $[\text{PNP}]_2[\text{B}_7\text{H}_7] \cdot 3\text{CH}_3\text{CN}$  were obtained by diffusion of Et<sub>2</sub>O into a solution of  $[\text{PNP}]_2[\text{B}_7\text{H}_7]$  in CH<sub>3</sub>CN.

All measured crystals show comparable bond lengths for the anion, as evident from Table 3. The averaged bond lengths derived for the  $[\text{B}_7\text{H}_7]^{2-}$  anion are in agreement to an idealized anion with  $D_{5h}$  symmetry. This is in agreement to theoretical data as listed in Table 3 (for more details see the Supporting Information).

**Crystal Structures of Salts of the  $[\text{B}_7\text{H}_8]^-$  Anion.** The protonated anion  $[\text{B}_7\text{H}_8]^-$  was crystallized with different cations and studied by single-crystal X-ray diffraction resulting in different structures, solvates, and polymorphs. An overview on the two structures of highest quality is presented in Table 4 (for more details see the Supporting Information).

Crystals of  $[\text{PNP}][\text{B}_7\text{H}_8]$  and  $[\text{PPh}_4][\text{B}_7\text{H}_8]$  were obtained by diffusion of Et<sub>2</sub>O into a solution of  $[\text{PNP}][\text{B}_7\text{H}_8]$  or  $[\text{PPh}_4][\text{B}_7\text{H}_8]$  in CH<sub>2</sub>Cl<sub>2</sub>, respectively.  $[\text{PNP}][\text{B}_7\text{H}_8]$  and  $[\text{PPh}_4][\text{B}_7\text{H}_8]$  were prepared as described in the Experimental Section.

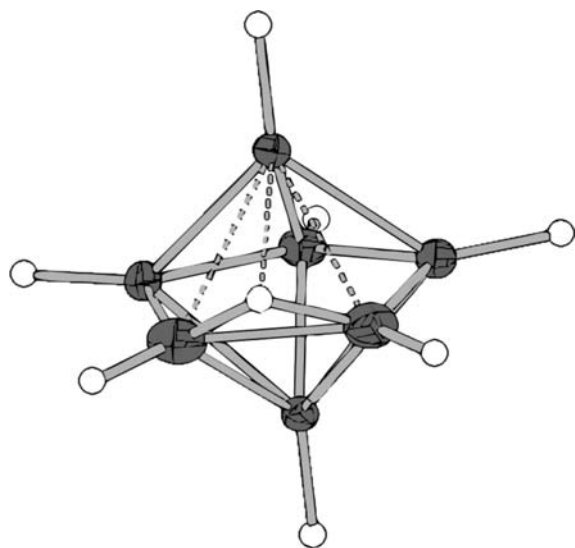


**Figure 8.** Structure of the  $[\text{B}_7\text{H}_8]^-$  anion in  $[\text{N}(n\text{-Bu}_4)][\text{B}_7\text{H}_8]$  with 50% probability thermal ellipsoids for the B atoms.

**Table 5.** Bond Lengths in the Anions in  $[\text{N}(n\text{-Bu}_4)][\text{B}_7\text{H}_8]^a$

$d$ , Å	anion1	anion2	average values <sup>b</sup>	calculated <sup>c</sup>	calculated <sup>d</sup>
$\text{B}_1\text{--B}_2$	2.024(4)	2.003(4)	2.014{8}	2.086	2.032
$\text{B}_1\text{--B}_3$	2.032(4)	1.997(4)	2.014{8}	2.086	2.032
$\text{B}_1\text{--B}_4$	1.763(3)	1.764(4)	1.762{2}	1.754	1.748
$\text{B}_1\text{--B}_6$	1.757(4)	1.765(3)	1.762{2}	1.754	1.748
$\text{B}_1\text{--B}_5$	1.778(4)	1.775(4)	1.777{2}	1.779	1.778
$\text{B}_7\text{--B}_2$	1.820(4)	1.803(4)	1.822{7}	1.805	1.798
$\text{B}_7\text{--B}_3$	1.836(4)	1.828(4)	1.822{7}	1.805	1.798
$\text{B}_7\text{--B}_4$	1.809(4)	1.816(3)	1.809{3}	1.841	1.827
$\text{B}_7\text{--B}_6$	1.808(3)	1.802(4)	1.809{3}	1.841	1.827
$\text{B}_7\text{--B}_5$	1.777(3)	1.797(4)	1.787{10}	1.802	1.799
$\text{B}_2\text{--B}_3$	1.715(4)	1.686(5)	1.701{15}	1.745	1.724
$\text{B}_2\text{--B}_6$	1.647(4)	1.633(4)	1.639{6}	1.678	1.673
$\text{B}_3\text{--B}_4$	1.650(4)	1.625(4)	1.639{6}	1.678	1.673
$\text{B}_4\text{--B}_5$	1.635(4)	1.640(4)	1.639{1}	1.646	1.638
$\text{B}_6\text{--B}_5$	1.640(4)	1.640(4)	1.639{1}	1.646	1.638

<sup>a</sup> Labeling, see Figure 1. <sup>b</sup> Calculated with Origin 7G SR2 (v7.0394), in brackets: error of the measurement; in curly brackets: statistical error. <sup>c</sup> B3LYP/6-311++g(d,p). <sup>d</sup> MP2(FULL)/6-31G\*<sup>24</sup>

A mixture of  $[\text{N}(n\text{-Bu}_4)][\text{B}_7\text{H}_8]$  and  $[\text{N}(n\text{-Bu}_4)][\text{B}_6\text{H}_7]$  was prepared by the addition aqueous HCl (conc.) at 273 K to the basic reaction solution after removal of the organic solvents and separation of  $[\text{B}_{12}\text{H}_{12}]^{2-}$  and  $[\text{B}_{10}\text{H}_{10}]^{2-}$  (Scheme 2, step V).  $[\text{N}(n\text{-Bu}_4)]\text{--}[\text{B}_7\text{H}_8]$  and  $[\text{N}(n\text{-Bu}_4)]\text{--}[\text{B}_6\text{H}_7]$  precipitated as colorless solids and were dried in vacuum. Crystals of  $[\text{N}(n\text{-Bu}_4)][\text{B}_7\text{H}_8]$  were obtained by diffusion of  $\text{Et}_2\text{O}$  into a solution of the aforementioned mixture in  $\text{CH}_2\text{Cl}_2$ . In the structure of  $[\text{N}(n\text{-Bu}_4)][\text{B}_7\text{H}_8]$  two symmetry independent anions and cations are found. Anion 1 has smaller thermal ellipsoids, and the bond lengths between  $\text{B}_1\text{--B}_2$  and  $\text{B}_1\text{--B}_3$  are slightly longer compared to anion 2. A view of this anion 1 is shown in Figure 8.

The bridging proton was found, as expected, in the residual electron density as the strongest peak near B2 and B3. Those boron atoms show the longest bond distance for the equatorial boron atoms. The distances between  $\text{B}_1\text{--B}_2$  and  $\text{B}_1\text{--B}_3$  are the

**Table 6.** Differences of Bond Lengths in  $[\text{N}(n\text{-Bu}_4)][\text{B}_7\text{H}_8]$  and  $[\text{N}(n\text{-Bu}_4)]_2[\text{B}_7\text{H}_7]$

$d$ , Å	$[\text{N}(n\text{-Bu}_4)][\text{B}_7\text{H}_8]^a$	$\Delta(d, \text{Å})^b$
$\text{B}_1\text{--B}_2, \text{B}_1\text{--B}_3$	2.014	0.193
$\text{B}_1\text{--B}_4, \text{B}_1\text{--B}_6$	1.762	−0.059
$\text{B}_1\text{--B}_5$	1.777	−0.044
$\text{B}_7\text{--B}_2, \text{B}_7\text{--B}_3$	1.822	0.001
$\text{B}_7\text{--B}_4, \text{B}_7\text{--B}_6$	1.809	−0.012
$\text{B}_7\text{--B}_5$	1.787	−0.034
$\text{B}_2\text{--B}_3$	1.701	0.052
$\text{B}_2\text{--B}_6, \text{B}_3\text{--B}_4$	1.639	−0.010
$\text{B}_4\text{--B}_5, \text{B}_6\text{--B}_5$	1.639	−0.010

<sup>a</sup> Values on average, calculated with Origin 7G SR2 (v7.0394). <sup>b</sup> Difference of bond length of  $[\text{N}(n\text{-Bu}_4)][\text{B}_7\text{H}_8]$  and  $[\text{N}(n\text{-Bu}_4)]_2[\text{B}_7\text{H}_7]$ .

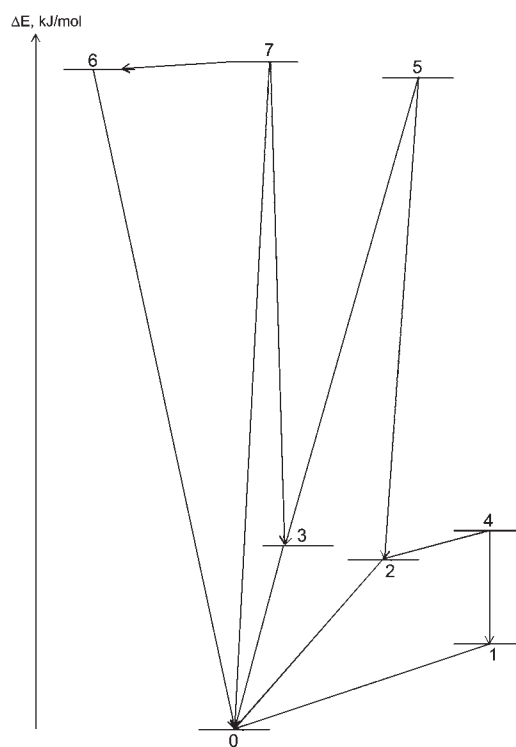


**Figure 9.** Correlation of minima and transition states of the monoanion  $[\text{B}_7\text{H}_8]^-$ , labeling see Table 7 (for more details see the Supporting Information).

longest ones in the anions. In Table 5 the bond lengths of the anions in  $[\text{N}(n\text{-Bu}_4)][\text{B}_7\text{H}_8]$  are summarized.

The bond length between B2 and B3, where the bridging proton is located, significantly differs from the bond lengths of the deprotonated form of the B<sub>7</sub>-cluster (for B<sub>2</sub>–B<sub>3</sub> in  $[\text{B}_7\text{H}_8]^-$  1.701 Å; and for B<sub>2</sub>–B<sub>3</sub> in  $[\text{B}_7\text{H}_7]^{2-}$  1.649 Å). The bonds between B<sub>1</sub>–B<sub>2</sub> and B<sub>1</sub>–B<sub>3</sub> are with 2.014(8) Å very long. In comparison, the bond distances in the  $[\text{B}_7\text{H}_7]^{2-}$  anion between axial and equatorial boron atoms are 1.821(2) Å. An overview of the differences in the bond lengths is shown in Table 6.

Some of the bonds in  $[\text{B}_7\text{H}_8]^-$  are shorter than in  $[\text{B}_7\text{H}_7]^{2-}$  (in Table 6 marked with “−”). This effect is most markedly for the bonds between B<sub>1</sub>–B<sub>4</sub> and B<sub>1</sub>–B<sub>6</sub>, which are shorter by 0.059 Å compared to those in the  $[\text{B}_7\text{H}_7]^{2-}$  anion. In summary,

Table 7. Minima and Transition States of  $[\text{B}_7\text{H}_8]^-$ 

No.	P.G.	$n^a$	$\Delta E,^b$ kJ/mol	$\Delta E_{\text{korrr}},^b$ kJ/mol	$\Delta E,^c$ kJ/mol	$\Delta E_{\text{korrr}},^d$ kJ/mol	$c,d$	comment
0	$C_s$	10	0	0	0	0	t445, $C_s$ (2)	
1	$C_{2v}$	5	10.4	9.3	10.5	10.5	b44, $C_{2v}$ (3)	equalize $B_{\text{ax}}$
2	$C_2$	10	61.2	54.1				equalize $B_{\text{ax}}$ equalize $B_{\text{eq}}$ substitution $H_{\text{eq}}$
3	$C_s$	10	62.7	55.7	80.8	72.4	b45, $C_s$ (4)	equalize $B_{\text{eq}}$
4	$C_{2v}$	5	66.5	57.8	69.9	62.3	v4, $C_{2v}$ (5)	equalize $B_{\text{ax}}$ equalize $B_{\text{eq}}$ substitution $H_{\text{eq}}$
5	$C_{2v}$	5	145.1	130.6				equalize $B_{\text{ax}}$ substitution $H_{\text{eq}}$
6	$C_s$	10	146.8	131.3	173.6	160.2	v5, $C_s$ (6)	equalize $B_{\text{eq}}$ substitution $H_{\text{ax}}$
7	$C_s$	10	146.9	131.2				substitution $H_{\text{ax}}$

<sup>a</sup>  $n$  = number of minima/transition states in the cluster. <sup>b</sup> B3LYP/6-311++g(d,p), this work. <sup>c</sup> MP2(frozen core)/6-31G\*\*//6-31G\*. <sup>d</sup> MP2(FC)/6-31G\*\*//6-31G\*\*+ZPE(3-21G).<sup>24</sup>

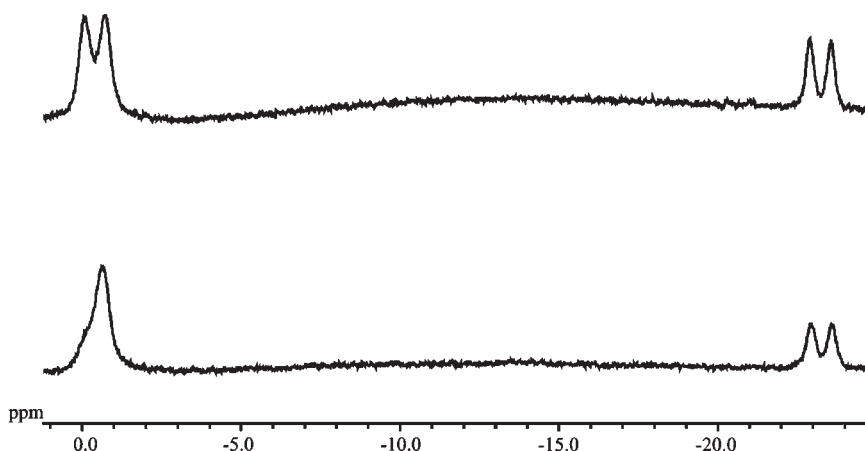


Figure 10.  $^{11}\text{B}$  NMR spectra of  $\text{Na}_2[\text{B}_7\text{H}_7]$  in  $\text{D}_2\text{O}$  under basic conditions (top) and after 3 h under neutral conditions (bottom).

the pentagonal bipyramid is expanded at B1B2B3 and compressed at B1B4B5 and B1B5B6 upon protonation.

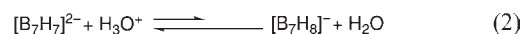
**Theoretical Aspects.** The calculations presented herein for  $[\text{B}_7\text{H}_7]^{2-}$  and  $[\text{B}_7\text{H}_8]^-$  are in close agreement to earlier studies (Table 7 and the Supporting Information).<sup>24</sup> In Figure 9 the minima and the transition states depending on the relative energy differences are depicted (for the calculated structures see the Supporting Information).

The dynamic behavior of  $[\text{B}_7\text{H}_8]^-$  in solution as evident from the NMR spectra in Figure 4 is in agreement with the small activation energies for the transition states 1–4 as depicted in Figure 9. Hence, the two axial boron atoms as well as the five equatorial boron atoms are NMR spectroscopically equivalent at room temperature. Already at 273 K the five  $B_{\text{eq}}$  show 3 doublets with an intensity of 2:2:1. In this case the migration of  $H_{\mu}$  around the five membered ring stops. The signal of the two  $B_{\text{ax}}$  shows even at 213 K no further split-up. The flapping of  $H_{\mu}$  upward and downward to the fivering cannot be frozen out, because the transition state 1 is only 10 kJ/mol higher in energy than the ground state. The transition states 2 and 4 allow a substitution of  $H_{\mu}$  and  $H_{\text{eq}}$ . An exchange of  $H_{\mu}$  and  $H_{\text{ax}}$  is possible via the

transition states 6 and 7, but these states are, in comparison to the transition 2 and 4, high in energy, as shown in Table 7.

The calculated transition states were supported by substitution experiments of H against D in aqueous medium.  $[\text{PPh}_4]_2[\text{B}_7\text{H}_7]$  was dissolved in  $\text{CH}_2\text{Cl}_2/\text{NPr}_3$  and a 0.1 M NaOH solution was added.  $\text{Na}[\text{BPh}_4]$ , in 1.0 M NaOH was added, and after filtration the aqueous layer was separated.  $\text{K}_2\text{CO}_3$  was added and after filtration of  $\text{K}[\text{BPh}_4]$  the aqueous solution was evaporated to dryness. In  $\text{D}_2\text{O}$ , under basic conditions, no substitution of H and D was observed (Figure 10). After neutralization with  $\text{CO}_2$  ( $\approx$  pH 7), a substitution of the five equatorial H atoms by D atoms was observed after a few hours.

For the five equatorial boron atoms a signal without coupling to H at pH 7 was observed. The two axial protons do not show a substitution from H to D as evident from the  $^{11}\text{B}$  NMR spectrum. At pH 7 in aqueous solution an equilibrium between  $[\text{B}_7\text{H}_7]^{2-}$  and  $[\text{B}_7\text{H}_8]^-$  exists, as depicted in eq 2.



The selective substitution of the 5  $B_{\text{eq}}$  is in agreement with the theoretical results. The substitution of  $B_{\text{ax}}$  is not



observed, because the transition states 6 and 7 are too high in energy.

## CONCLUSIONS

We have developed an improved synthesis for salts of the dianionic *closo*-cluster  $[\text{B}_7\text{H}_7]^{2-}$ . The monoanion  $[\text{B}_7\text{H}_8]^-$  is easily prepared from the dianion in quantitative yield. Both compounds were characterized by NMR spectroscopy. The dynamic NMR behavior of  $[\text{B}_7\text{H}_8]^-$  was analyzed and compared with theoretical calculations. Experimental data are in agreement with calculated values. Structures of  $[\text{B}_7\text{H}_7]^{2-}$  as well as  $[\text{B}_7\text{H}_8]^-$  with various cations were determined by single X-ray diffraction. The structure of  $[\text{B}_7\text{H}_7]^{2-}$  fills the gap of published structures in the series of *closo*-hydro-borates  $[\text{B}_n\text{H}_n]^{2-}$  ( $n = 6-12$ ). Currently, we are exploring the chemistry of the  $[\text{B}_7\text{H}_7]^{2-}$  anion as a starting material for the preparation of larger anionic boron clusters.

## ASSOCIATED CONTENT

**S Supporting Information.** NMR spectra for starting material and more details about the crystal structures and the calculations. This material is available free of charge via the Internet at <http://pubs.acs.org>.

## AUTHOR INFORMATION

### Corresponding Author

\*E-mail: [edbern@uni-wuppertal.de](mailto:edbern@uni-wuppertal.de).

## ACKNOWLEDGMENT

The authors thank Professor H. Willner for generous support and helpful discussions, Professor R. Eujen for help by NMR problems, and PD Dr. M. Finze for helpful discussions.

## REFERENCES

- (1) Hawthorne, M. F.; Pitochelli, A. R. *J. Am. Chem. Soc.* **1959**, *81*, 5519.
- (2) Boone, J. L. *J. Am. Chem. Soc.* **1964**, *86*, 5036.
- (3) Klanberg, F.; Eaton, D. R.; Guggenberger, L. J.; Muettterties, E. L. *Inorg. Chem.* **1967**, *6*, 1271.
- (4) Klanberg, F.; Muettterties, E. L. *Inorg. Chem.* **1966**, *5*, 1955.
- (5) Pitochelli, A. R.; Hawthorne, F. M. *J. Am. Chem. Soc.* **1960**, *82*, 3228.
- (6) Preetz, W.; Peters, G. *Eur. J. Inorg. Chem.* **1999**, 1831.
- (7) Volkov, O.; Paetzold, P. *J. Organomet. Chem.* **2003**, *680*, 301.
- (8) Sivaev, I. B.; Bregadze, V. I.; Sjöberg, S. *Collect. Czech. Chem. Commun.* **2002**, *67*, 679.
- (9) Schaeffer, R.; Johnson, Q.; Smith, G. S. *Inorg. Chem.* **1965**, *4*, 917.
- (10) Kuznetsov, I. Y.; Vinitskii, D. M.; Solntsev, K. A.; Kuznetsov, N. T.; Butman, L. A. *Zh. Neorg. Khim.* **1987**, *32*, 3112.
- (11) Guggenberger, L. J. *Inorg. Chem.* **1969**, *8*, 2771.
- (12) Guggenberger, L. J. *Inorg. Chem.* **1968**, *7*, 2260.
- (13) Kaczmarczyk, A.; Dobrott, R. D.; Lipscomb, W. N. *Proc. Natl. Acad. Sci. U.S.A.* **1962**, *48*, 729.
- (14) Dobrott, R. D.; Lipscomb, W. N. *J. Chem. Phys.* **1962**, *37*, 1779.
- (15) Kraus, F.; Albert, B. *Z. Anorg. Allg. Chem.* **2005**, *631*, 152.
- (16) Volkov, O.; Dirk, W.; Englert, U.; Paetzold, P. *Z. Anorg. Allg. Chem.* **1999**, *625*, 1193.
- (17) Wunderlich, J. A.; Lipscomb, W. N. *J. Am. Chem. Soc.* **1960**, *82*, 4427.
- (18) Tiritiris, I.; Schleid, T. *Z. Anorg. Allg. Chem.* **2003**, *629*, 1390.
- (19) For an overview of published crystal structures of  $[\text{B}_n\text{H}_n]^{2-}$  ( $n = 6-12$ ) see the Supporting Information.
- (20) Housecroft, C. E.; Snaith, R.; Moss, K.; Mulvey, R. E.; O'Neill, M. E.; Wade, K. *Polyhedron* **1985**, *4*, 1875.
- (21) Dewkett, W. J.; Grace, M.; Beall, H. *J. Inorg. Nucl. Chem.* **1971**, *33*, 1279.
- (22) Bader, R. F. W.; Legare, D. A. *Can. J. Chem.* **1992**, *70*, 657.
- (23) Joseph, J.; Gimarc, B. M.; Zhao, M. *Polyhedron* **1993**, *12*, 2841.
- (24) Mebel, A. M.; Charkin, O. P.; Schleyer, P. v. R. *Inorg. Chem.* **1993**, *32*, 469.
- (25) Mebel, A. M.; Schleyer, P. v. R.; Najafian, K.; Charkin, O. P. *Inorg. Chem.* **1998**, *37*, 1693.
- (26) Wrackmeyer, B. *Z. Naturforsch., B: Chem. Sci.* **2005**, *60*, 955.
- (27) Bernhardt, B.; Brauer, D.; Finze, M.; Willner, H. *Angew. Chem.* **2007**, *119*, 2985.
- (28) Bernhardt, E.; Brauer, D. J.; Finze, M.; Willner, H. *Angew. Chem., Int. Ed.* **2007**, *46*, 2927.
- (29) *CrysAlisPro*, version 1.171.33.42; Oxford Diffraction Ltd: Oxford, U. K.
- (30) Kohn, W.; Sham, L. J. *Phys. Rev. A* **1965**, *140*, 1133.
- (31) Becke, A. D. *Phys. Rev. B* **1988**, *38*, 3098.
- (32) Lee, C.; Yang, W.; Parr, R. G. *Phys. Rev. B* **1988**, *41*, 785.
- (33) Becke, A. D. *J. Chem. Phys.* **1993**, *98*, 5648.
- (34) Frisch, M. J.; Trucks, G. W.; Schlegel, H. B.; Scuseria, G. E.; Robb, M. A.; Cheeseman, J. R.; Montgomery, J. A., Jr.; Vreven, T.; Kudin, K. N.; Burant, J. C.; Millam, J. M.; Iyengar, S. S.; Tomasi, J.; Barone, V.; Mennucci, B.; Cossi, M.; Scalmani, G.; Rega, N.; Petersson, G. A.; Nakatsuji, H.; Hada, M.; Ehara, M.; Toyota, K.; Fukuda, R.; Hasegawa, J.; Ishida, M.; Nakajima, T.; Honda, Y.; Kitao, O.; Nakai, H.; Klene, M.; Li, X.; Knox, J. E.; Hratchian, H. P.; Cross, J. B.; Adamo, C.; Jaramillo, J.; Gomperts, R.; Stratmann, R. E.; Yazyev, O.; Austin, A. J.; Cammi, R.; Pomelli, C.; Ochterski, J. W.; Ayala, P. Y.; Morokuma, K.; Voth, G. A.; Salvador, P.; Dannenberg, J. J.; Zakrzewski, V. G.; Dapprich, S.; Daniels, A. D.; Strain, M. C.; Farkas, O.; Malick, D. K.; Rabuck, A. D.; Raghavachari, K.; Foresman, J. B.; Ortiz, J. V.; Cui, Q.; Baboul, A. G.; Clifford, S.; Cioslowski, J.; Stefanov, B. B.; Liu, G.; Liashenko, A.; Piskorz, P.; Komaromi, I.; Martin, R. L.; Fox, D. J.; Keith, T.; M. A. Al-Laham, Peng, C. Y.; Nanayakkara, A.; Challacombe, M.; Gill, P. M. W.; Johnson, B.; Chen, W.; Wong, M. W.; Gonzalez, C.; Pople, J. A. *Gaussian 03*, Revision B.05; Gaussian, Inc.: Wallingford, CT, 2003.
- (35) London, F. *J. Phys. Radium* **1937**, *8*, 397.
- (36) McWeeny, R. *Phys. Rev.* **1962**, *126*, 1028.
- (37) Ditchfield, R. *Mol. Phys.* **1974**, *27*, 789.
- (38) Dodds, J. L.; McWeeny, R.; Sadlej, A. J. *Mol. Phys.* **1980**, *41*, 1419.
- (39) Wolinski, K.; Hinton, J. F.; Pulay, P. *J. Am. Chem. Soc.* **1990**, *112*, 8251.
- (40) Helgaker, T.; Watson, M.; Handy, N. C. *J. Chem. Phys.* **2000**, *113*, 9402.
- (41) Sychrovsky, V.; Grafenstein, J.; Cremer, D. *J. Chem. Phys.* **2000**, *113*, 3530.
- (42) Barone, V.; Peralta, J. E.; Contreras, R. H.; Snyder, J. P. *J. Phys. Chem. A* **2002**, *106*, 5607.
- (43) Rienstra-Kiracofe, J. C.; Tschumper, G. S.; Schäfer, H. F.; Nandi, S.; Ellison, G. B. *Chem. Rev.* **2002**, *102*, 231.
- (44) Gonzales, C.; Schlegel, H. B. *J. Chem. Phys.* **1989**, *90*, 2154.
- (45) Gonzales, C.; Schlegel, H. B. *J. Phys. Chem.* **1990**, *94*, 5523.
- (46) Ruff, J. K.; Schlientz, W. *J. Inorg. Synth.* **1974**, *15*, 84.
- (47) Bublitz, D.; Franken, A.; Preetz, W.; Thomsen, H. *Z. Naturforsch.* **1996**, *51b*, 744.
- (48) Albert, B. *Angew. Chem.* **1998**, *110*, 1135.
- (49) Albert, B.; Hofmann, K. *Z. Anorg. Allg. Chem.* **1999**, *625*, 709.
- (50) Stibr, B.; Tok, O. L.; Milius, W.; Bakardjiev, M.; Holub, J.; Hnyk, D.; Wrackmeyer, B. *Angew. Chem., Int. Ed.* **2002**, *41*, 2126.
- (51) Schlüter, F.; Bernhardt, E. *Z. Anorg. Allg. Chem.* **2010**, *636*, 2462.

- (52) Stibr, B. *Chem. Rev.* **1992**, *92*, 225.
- (53) Mutseneck, E. V.; Wadepohl, H.; Enders, M.; Kudinov, A. R.; Siebert, W. *Eur. J. Inorg. Chem.* **2010**, 2911.
- (54) Hosmane, N. S.; Maguire, J. A. In *Comprehensive Organometallic Chemistry III (COMC-III)*; Crabtree, R. H., Mingos, D. M. P, Eds.; Elsevier: Oxford, 2006; Vol. 3, p 175.
- (55) Horner, L.; Mummmenthey, G.; Moser, H.; Beck, P. *Chem. Ber.* **1966**, *99*, 2782.